Supplementary Information

Enhanced cyclic stability of TiO_2-coated V_2O_5 nanorods through a surface sol-gel process for lithium ion battery applications

Shuang Tian,[a] An Xing,[a] Huang Tang,[a] Zhihao Bao*[a] and Guangming Wu*[a]

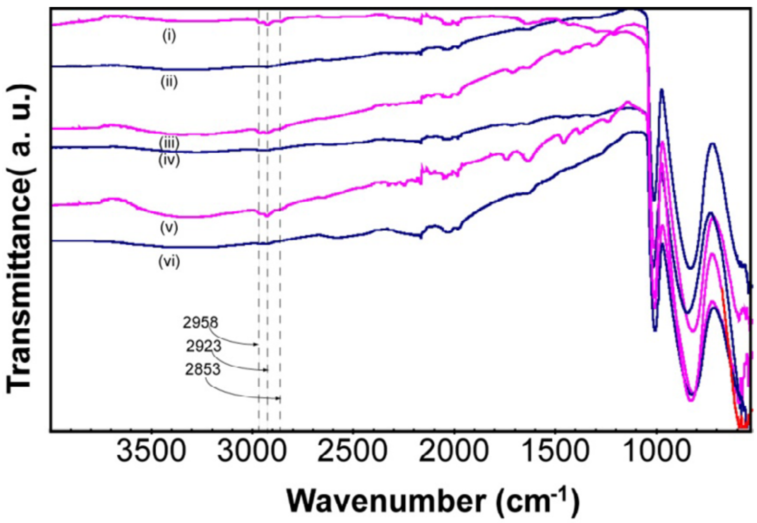

Figure S1. FTIR spectra of V_2O_5 nanorods after (i) first chemisorption of Ti(O-nBu)$_4$, (ii) first hydrolysis in water, (iii) second chemisorption of Ti(O-nBu)$_4$, (iv) second hydrolysis in water, (v) third chemisorption of Ti(O-nBu)$_4$, and (vi) third hydrolysis in water.

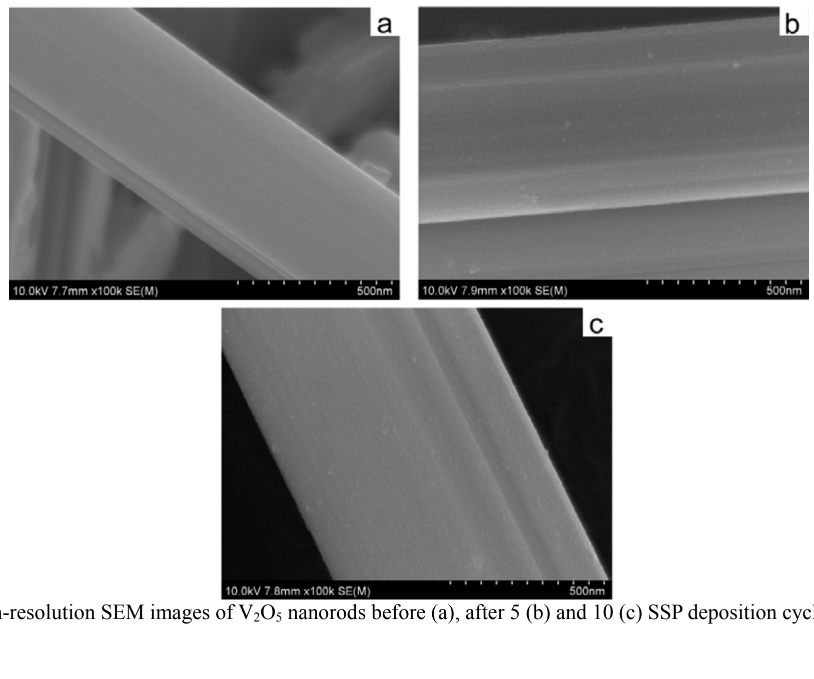

Figure S2. High-resolution SEM images of V_2O_5 nanorods before (a), after 5 (b) and 10 (c) SSP deposition cycles, respectively

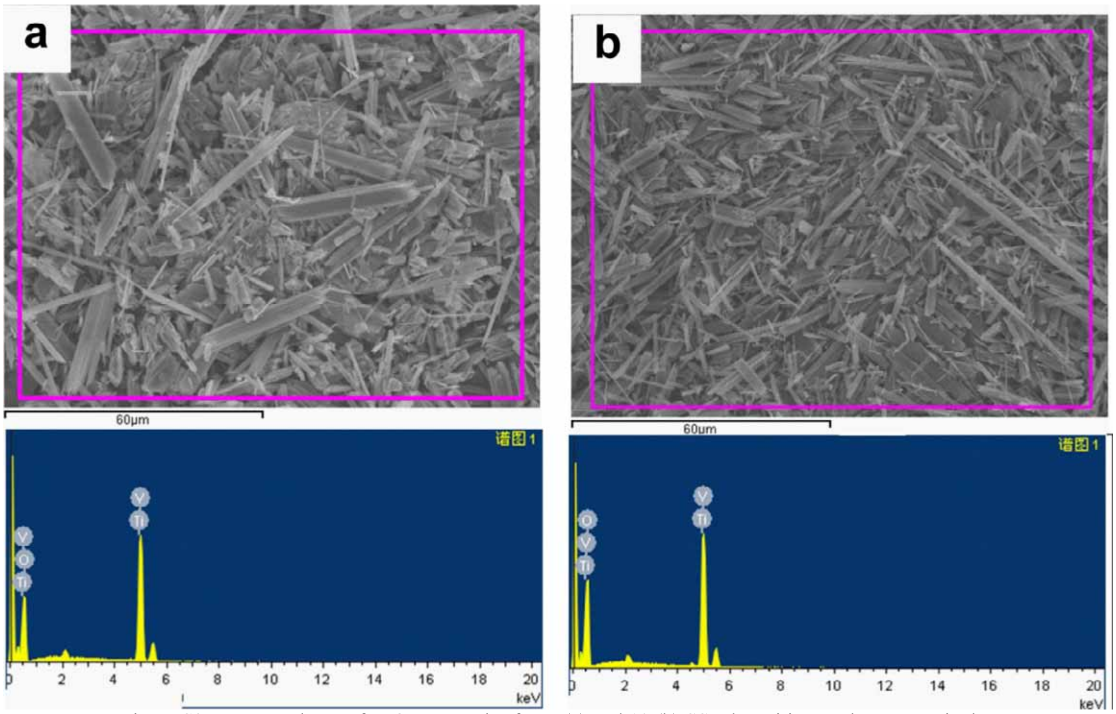

Figure S3 . EDX analyses of V_2O_5 nanorods after 5 (a) and 10 (b) SSP deposition cycles, respectively.

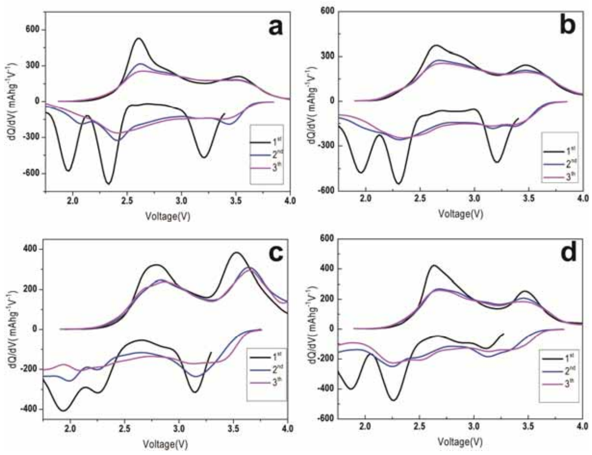

Figure S4. dQ/dV versus voltage profiles of the electrodes based on V_2O_5 powder (a) , bare nanorods (b), nanorods after 5 SSP deposition cycles (c) , and nanorods after 10 SSP deposition cycles (d), respectively.

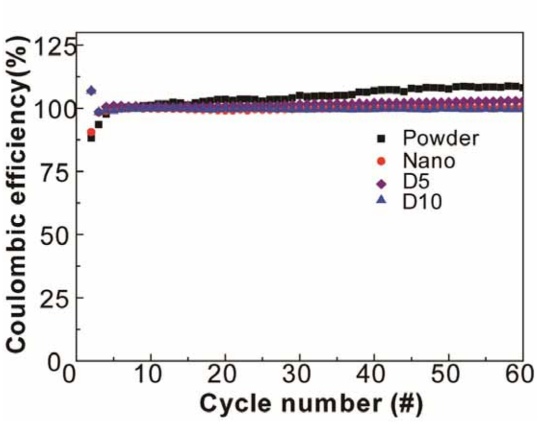

Figure S5. Plots of the Coulombic efficiencies of the electrodes versus the cycle number.

Table S1. Summary of the electrochemical performance of the modified V_2O_5 electrodes in the recent works.

Reference No.	Materials	Specific current	Capacity after n cycles (mAh g-1)
This work	TiO_2-coated V_2O_5	30 mA g^{-1}	251 (after 60 cycles)
1	spherically shaped dense V_2O_5	29.4 mA g^{-1}	263 (after 20 cycles)
2	ZrO_2-Doped V_2O_5 Amorphous Powders	294 mA g^{-1}	222 (after 50 cycles)
3	V_2O_5/polypyrrole	0.1C	225.4(after 50 cycles)
4	Cu-doped V_2O_5	80 mA g^{-1}	220 (after 45 cycles)
5	Al-Intercalated V_2O_5	35 mA g^{-1}	231(after 50 cycles)
6	Three-Dimensional Vanadium Oxide	300 mA g^{-1}	219(after 50 cycles)
7	V_2O_5 microspheres	10C	130(after 100 cycles)
8	yolk–shell V_2O_5 powders	1000 mA g^{-1}	201(after 100 cycles)
9	V_2O_5 − polypyrrole	40 mA g-1	187(after 100 cycles)
10	V_2O_5 films	0.025 mA cm^{-2}	200(after 40 cycles)

Reference:

1,Ko, Y. N.; Kim, J. H.; Choi, S. H.; Kang, Y. C. J. Power Sources 2012, 211, 84
2 ,Y. N. Ko, S. H. Choi, Y. C. Kang and S. B. Park, ACS Appl. Mater. Interfaces, 2013, 5, 3234
3,X.Z. Ren, C. Shi, P. Zhang, Y.K. Jiang, J.H. Liu, Q.L. Zhang, Mater. Sci. and Eng. B, 177 (2012), 929
4,D. Zhu, H. Liu, L. Lv, Y.D. Yao, W.Z. Yang, Scripta Materialia, 59 (2008), p. 642
5,Cheah, Y. L.; Aravindan, V.; Madhavi, S. ACS Appl. Mater. Interfaces 2012, 4 (6) 3270–3277
6,A. Q. Pan, H. B. Wu, L. Yu, T. Zhu and X. W. Lou, ACS Appl.Mater. Interfaces, 2012, 4, 3874
7,Zhang, C.; Chen, Z.; Guo, Z.; Lou, X. W. Energy Environ. Sci. 2013, 6, 974−978.
8, Ko, You Na; Kang, Yun Chan; Park, Seung Bin, Nanoscale. 2013,5, 8899-8903
9, L. Noerochim, J. Z. Wang, D. Wexler, Md. M. Rahman, J. Chen and H. K. Liu, J. Mater. Chem., 2012, 22, 11159;
10. V. Varadaraajan, B. C. Satishkumar, J. Nanda, and P. Mohanty, J. Power Sources,196, 10704 (2011)

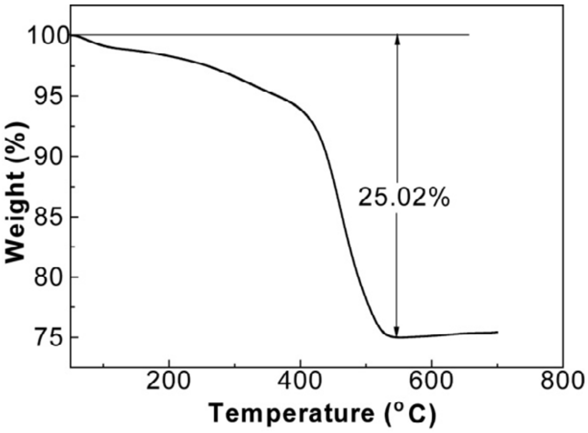

Figure S6. Thermogravimetric analysis of the V_2O_5(D5)/graphene composite thin film in air.